Supplementary Material

Tunable plasmonic enhancements in graphene based Fresnel zone plate lenses

Sunan Deng[1], Haider Butt[1,*], Kyle Jiang[1], Bruno Dlubak[2], Piran R. Kidambi, [3] Pierre Seneor[2], and Stephane Xavier[4], Ali K. Yetisen[5]

[1]School of Mechanical Engineering, University of Birmingham, Birmingham B15 2TT, UK
[2]Unité Mixte de Physique CNRS/Thales, 91767 Palaiseau, France, and Université Paris Sud, 91405 Orsay, France
[3]Department of Mechanical Engineering, Massachusetts Institute of Technology, Cambridge, MA 02139, USA
[4]Thales Research and Technology, 9 Department of Mechanical Engineering, Massachusetts Institute of Technology, Cambridge, MA 02139, USA 1767 Palaiseau, France
[5]Harvard-MIT Division of Health Sciences and Technology, Massachusetts Institute of Technology, Cambridge, Massachusetts 02139, USA
*Email: h.butt@bham.ac.uk

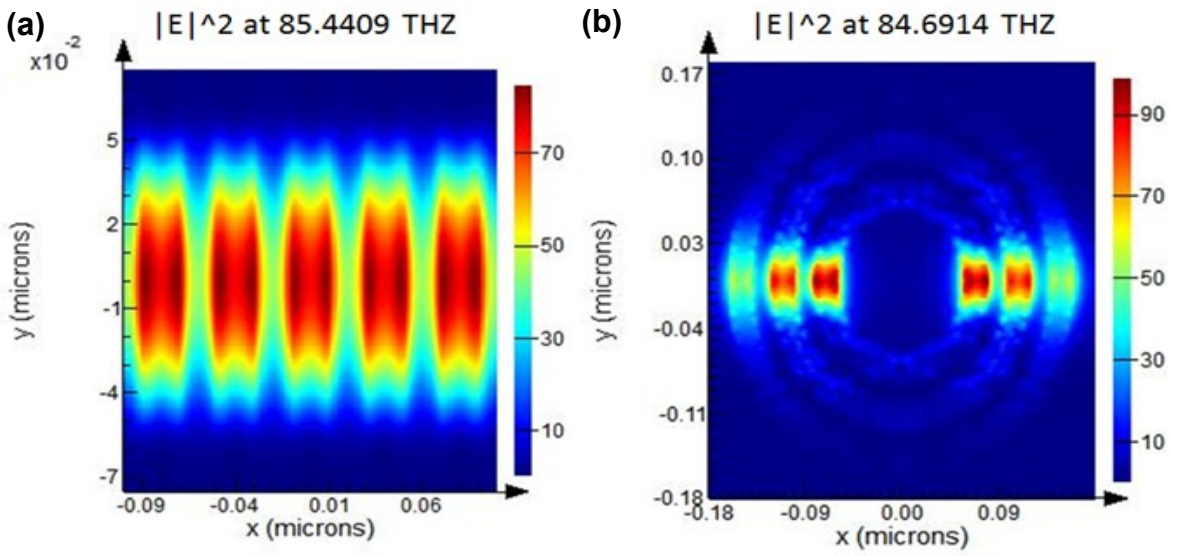

Figure S1. E-field distribution on xz plane of (a) a monolayer graphene ribbon array and (b) ring array at the resonance wavelength. For both situations, the graphene widths are 20 nm with a gap of 20 nm, at Fermi level 0.5 eV, with 2-20 μm broadband light shining from the y direction. The radii of the rings are 60-80 nm, 100-120 nm, and 140-160 nm, separately.

We performed a 3D simulation that shows that the rings array has analogous plasmonic effect as ribbons array (Figure S1). This figure shows the E-field distribution in xz plane of a monolayer graphene ribbons array (left) and rings array (right) at the resonance wavelength. The ribbons/rings were placed on the xz plane, with 2-20 μm broadband light shining from the y direction. In both cases, the width of the graphene patterns is 20 nm, gap 20 nm at a Fermi level of 0.5 eV. The radius of the smallest ring is 60-80 nm, and the biggest ring is 140-160 nm. The resonance wavelengths for ribbons array and rings array are

close, with 85.4 THz and 84.7 THz, respectively. In Liu, Penghong, et al. "Tunable terahertz optical antennas based on graphene ring structures." Applied Physics Letters 100.15 (2012): 153111, it was also confirmed that the first and second edge modes in perfect graphene rings are consistent with that in infinite-long graphene ribbons.

Meanwhile, 3D simulation is time and labor demanding. For example, 16 hours are needed for one cycle of calculations for a 3D area no more than 200×200 nm, while the minimum radius of the proposed lens in the paper is 20 μm. Hence, 2D simulations were performed.

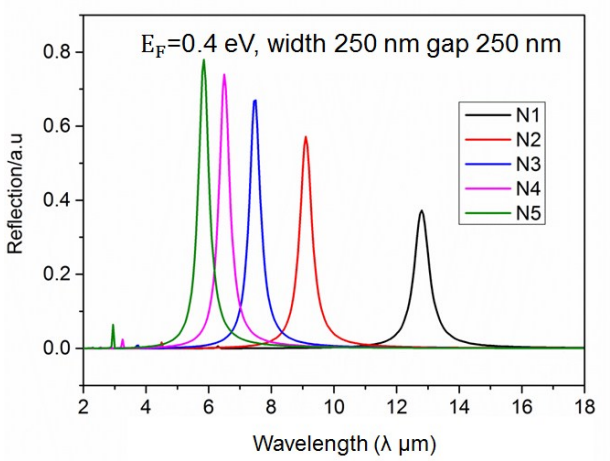

Figure S2. Reflection of graphene ribbons array with different layers, when both the width and gap of ribbons array are 250nm at a Fermi level of 0.4 eV.

Diffraction Efficiency Studies

When the gap is equal to the wavelength of incident light, the diffraction between the ribbons is so strong that the focal point and the power distribution pattern changes significantly (Figure S3). Figure S3a is the power flow distribution from a four-layer graphene FZP lens with a graphene ribbon width of 250 nm and a gap of 4.7 μm, equal to the incident light. Figure S3b demonstrates the power distribution, where two peaks can be observed. The first sharp peak is at y= 40 μm, which is about half of the theoretical focal length of 85 μm. The second peak near 80 μm should be the expected to be at the focal point, according to the FZP equation. In Figure 7b, more peaks can also be seen when y< 80 μm, which are caused by suborder diffraction and weaker than the value of focal points. Additionally, the small peaks neighboring the main peaks are in the range of y= [50, 60] μm. It is thought that the strong diffraction changes the position and the value of the suborder diffraction. Figure 8c is the power distribution when y= 40 μm, with the peak ratio I_1/I_2 =1.46. The FWHM of the peaks I_1 in 7c is only 3.9 μm, smaller than the incident

light, as compared with that in Figure 7c are 5.2-5.6 μm. Hence, higher diffraction does not necessary lead to higher peak ratio I_1/I_2.

Figure S3d compares peak ratio with incident light of 4.7 μm (resonance wavelength) and 4.9 μm (non-resonance wavelength) with different gaps when the single graphene ribbon parameters are the same (four-layer, Fermi level 0.7 eV, width 250 nm). The two cases share the same trend with varied gaps , which confirms that plasmonic effect has no contribution to the peak ratio change. To understand the interaction mechanism of the diffractions between and within FZP rings clearly, further studies are needed, which may pave the way for other graphene metamaterial devices.

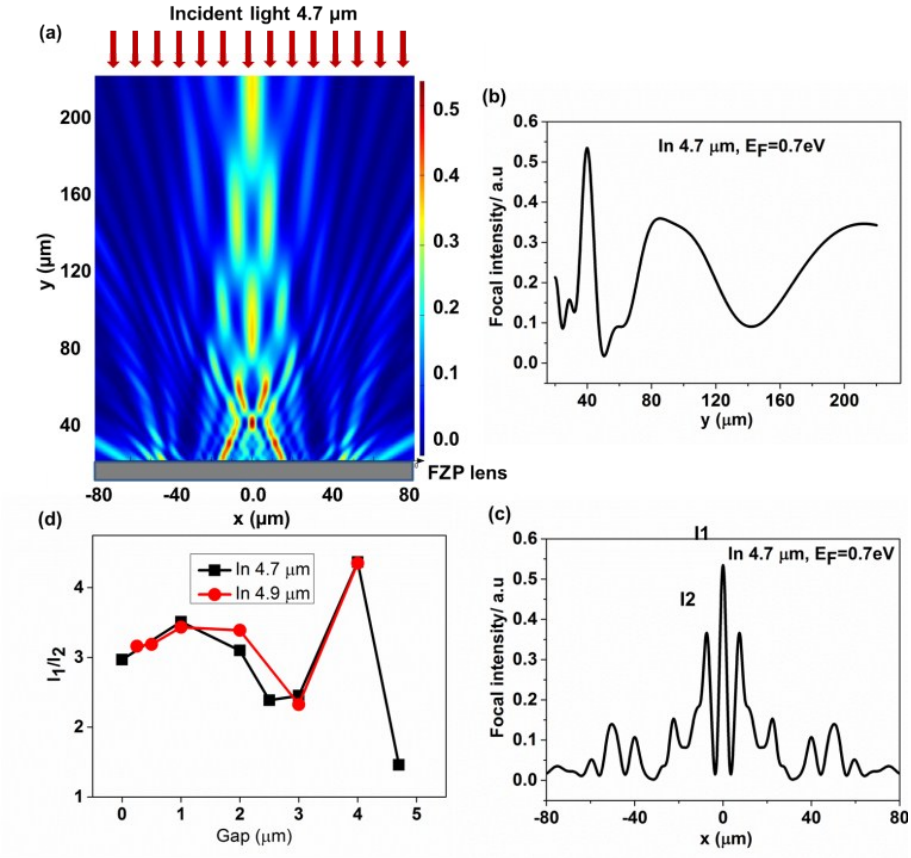

Figure S3. (a) Power flow distribution from four-layer graphene FZP lens, with graphene Fermi level of 0.7 eV, a width of 250 nm and a gap of 4.7 μm. Curves are extracted from (a) when (b) x=0 and (c) y=40 μm at the focal plane. (d) The peak ratio I_1/I_2 of focal point with different incident light when the gap of graphene ribbons varies.

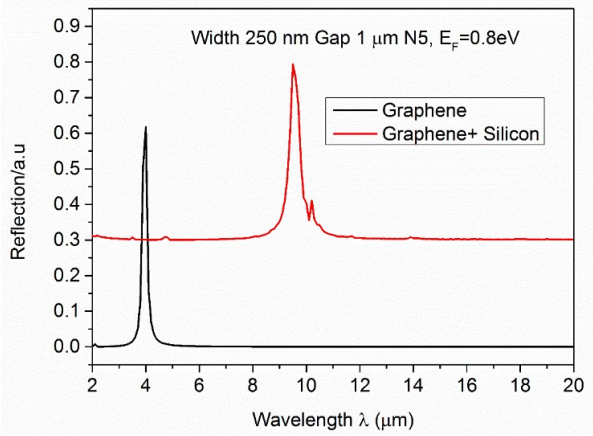

Figure S4. Reflections from suspended five-layer graphene ribbons array (black) and ribbons array on silicon substrate, with graphene ribbons width 250nm and gap 1 μm, Fermi level 0.8 eV.

Figure S4 shows that the silicon substrate will red shift the resonance wavelength owing to the damping led by the interactions between the graphene ribbons and the substrate. Additionally, the background reflection of the red curves is higher than the black one due to the reflections from silicon substrate.

Fabrication and Detection Limitations

The proposed plasmonic lenses were fabricated. Cylindrical geometry was chosen and fabricated on silicon substrate (Figure S5a). The cylindrical graphene FZP lens, with a central zone radius of 20 μm, was composed of an array with a nanoribbon width of 100 nm and a gap width of 250 nm. The enlarged optical imaging of the central zone is demonstrated in Figure S5b. It is suspected that the dark dots and bright dots in the central zone are defects and polymer deposits, respectively.

AFM measurements were carried out to measure the surface profile of the lens. Figures S5c,d show a clear distribution of the ribbon array. Figure S5d is the 3D version of (c), and it provides more details. The dust could reach as high as 25.98 nm and the thickness of the ribbons is ~2-3 nm. The dust could be contaminant during the fabrication process. Although the plasmonic lens was fabricated, there are many challenges to detect its tunability and lens enhancing effect for the following reasons:

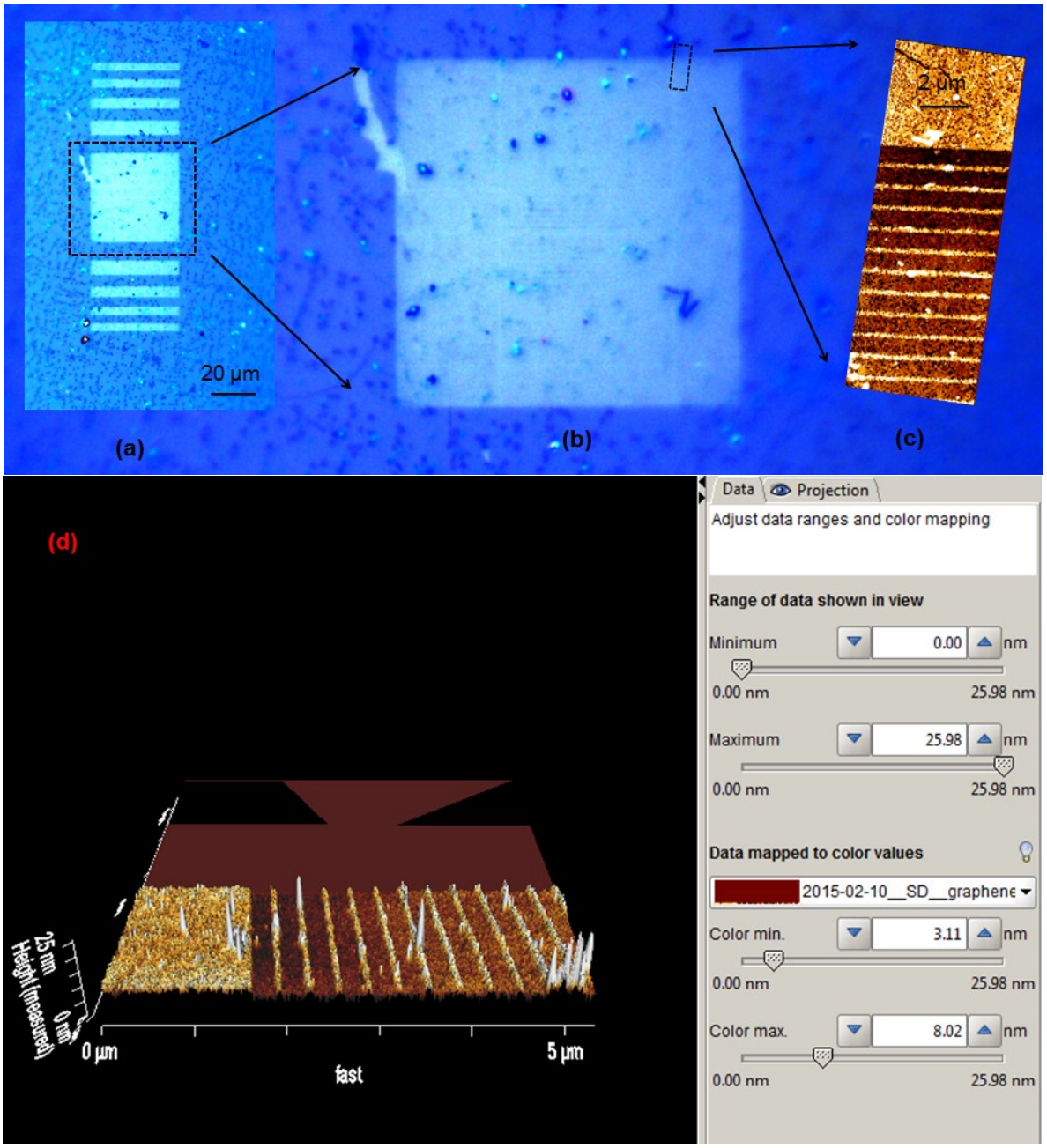

Figure S5. Cylindrical graphene FZP lens. (a) and (b) are optical microscopy images of the lens. (c) is 2D and (d) is 3D AFM images of the plasmonic lenses.

1. According to the simulation, graphene plasmonic lens works in mid-infrared to THz regime. However, it was difficult to find the corresponding imaging system at such wavelengths, as most of the imaging equipment works with visible or near infrared incident light. Additionally, the resolution of the conventional commercial infrared camera is low to detect such a micron size lens. The resolution of the

camera required should have a resolution of 40 μm (diameter for the central zone of the plasmonic FZP lens).

2. As compared with circular FZP lens, cylindrical FZP lens focuses light into a line instead of a point. Hence, detecting the lensing effect of cylindrical lenses is difficult as they produce a weaker focusing intensity.